ELSEVIER

Contents lists available at ScienceDirect

Soil Dynamics and Earthquake Engineering

journal homepage: www.elsevier.com/locate/soildyn





Calibration of the UBC3D-PLM soil model from Dilatometer Marchetti Test (DMT) for the liquefaction behaviour and cyclic resistance ratio (CRR) of sandy soils

F. Castelli^a, S. Grasso^b, V. Lentini^{a,*}, M.S.V. Sammito^a

ARTICLE INFO

Keywords: Liquefaction Horizontal stress index UBC3D-PLM model Cyclic resistance ratio

ABSTRACT

Seismic liquefaction is one of the most devastating natural hazards that can cause significant damage to structures and infrastructure. The liquefaction behaviour is simulated in the finite element code PLAXIS by the UBC3D-PLM constitutive model that is 3-D generalized formulation of the 2-D UBCSAND model developed at the University of British Colombia. The UBC3D-PLM model used in this work was successfully employed in many recent studies, e.g. to evaluate the liquefaction effects on the seismic soil–structure interaction, to assess the dynamic behaviour of earthen embankments built on liquefiable soil and to investigate the seismic performance of offshore foundations. Moreover, UBC3D-PLM model involves many input parameters to model the onset of the liquefaction phenomenon. Therefore, their determination becomes a crucial concern. Previous studies elaborated a specific formulation that requires the corrected Standard Penetration Test (SPT) blow counts as input. However, the Dilatometer Marchetti Test (DMT), compared to the SPT, is more sensitive to several factors that affect the liquefaction resistance such as aging, stress history, overconsolidation and horizontal earth pressure. For this reason, a new parameter selection procedure, which uses the horizontal stress index derived from DMT, was developed in this study.

The new relationships were applied for determining the initial parameters of the UBC3D-PLM model to describe the behavior of several liquefiable deposits located in eastern Sicily (Italy) that experienced destructive earthquakes in the past. For each site, the model was calibrated to the DMT-based liquefaction triggering curve, developed by combining DMT correlations with the current method based on SPT test, by the simulation of cyclic direct simple shear tests (CDSS). Finally, CDSS tests were performed by means of the CDSS device at the Soil Dynamics and Geotechnical Engineering Laboratory of the University "Kore" of Enna (Italy). This allowed to validate the applicability of the proposed procedure in simulating the liquefaction behavior of sandy soils.

1. Introduction

Several approaches and procedure are available from literature for liquefaction studies: laboratory tests [1,2], in situ tests [3,4], full-scale field tests [5], stress-based simplified procedures [6,7] and numerical models [8,9].

Laboratory testing requires high quality undisturbed samples of coarse-grained soils that can be obtained by expensive in situ ground freezing techniques [10]. An emerging lower cost alternative to ground freezing is the gel-push technology [11]. Simple and low-cost in situ testing commonly used to evaluate the liquefaction resistance of soil are

the Standard Penetration Tests (SPT) [6] and Cone Penetration Tests (CPT) [12]. As stated by several authors [13–16], the CPT and SPT are relatively insensitive to several factors affecting the liquefaction resistance such as aging, stress history, overconsolidation and horizontal earth pressure.

The liquefaction resistance can be also derived from the Seismic Dilatometer (SDMT) based on CRR-K $_D$ [17–20] and CRR-V $_S$ correlations [21]. However, Grasso et al. [22] evaluated the liquefaction potential for the city of Catania (Italy) using empirical correlations with SPT, CPT and SDMT, demonstrating that K_D is more sensitive to potential liquefaction behaviour than V_S .

E-mail addresses: francesco.castelli@unikore.it (F. Castelli), sgrasso@dica.unict.it (S. Grasso), valentina.lentini@unikore.it (V. Lentini), mariastellavanessa. sammito@unikore.it (M.S.V. Sammito).

^a Dept. of Engineering and Architecture, University "Kore" of Enna, Italy

^b Dept. of Civil Engr. and Architecture, University of Catania, Italy

^{*} Corresponding author.

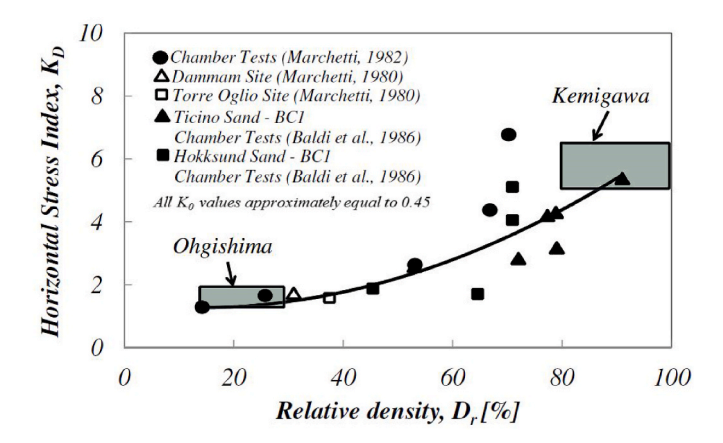


Fig. 1. Relationship between K_D and Dr [%] obtained by Reyna and Chameau [42] for normally consolidated uncemented sands and the Ohgishima and Kemigawa datapoints (rectangular areas) by Tanaka and Tanaka [43] (After Monaco et al. [17]; modified).

Marchetti [23] was the first to indicate the horizontal stress index, K_D , from the dilatometer Marchetti test (DMT), as a parameter able to provide the evaluation of liquefaction resistance. The K_D is defined as follow:

$$K_D = \frac{p_0 - u_0}{\sigma'_{v0}} \tag{1}$$

where p_0 is the corrected pressure required to begin the movement of a circular expandable steel membrane mounted on one side of the dilatometer, u_0 and σ'_{v_0} are the pre-insertion pore pressure and overburden stress, respectively [24].

Among the most significant factors supporting the use of the DMT for evaluation liquefaction resistance [17], the K_D from DMT is highly sensitive to stress history that is fundamental to predict the liquefaction behaviour. K_D reflects several stress history effects such as aging, horizontal earth pressure, structure and cementation. Moreover, Yu [25] developed a correlation between the K_D from DMT and the in situ state parameter, ξ_0 , that is strongly related to liquefaction resistance. These aspects encourage efforts to develop methods for evaluating liquefaction potential by DMT [26].

In the current engineering practice, the evaluation of liquefaction potential is carried out by simplified procedure based on the results of in situ tests [12,17,21]. However, the numerical simulations and the use of constitutive models are fundamental to simulate the seismic response of liquefiable soil [9]. Several constitutive models have been developed to capture the response of liquefiable soil [27–29]. The UBC3D-PLM model, implemented in the finite element code PLAXIS (Bentley), is an effective stress elasto-plastic model that describes the liquefaction behavior of sands and silty sands under cyclic loading [30]. Its formulation is based on the UBCSAND model developed by Puebla et al. [31] and Beaty and Byrne [32].

The main contribution of this paper is to suggest specific correlations between the parameters of the UBC3D-PLM model and the K_D from DMT. The adopted procedure is similar to the one used by Monaco et al. [17] and Grasso and Maugeri [18] for evaluating the cyclic resistance ratio (CRR) from DMT to be used according to the simplified procedure originally developed by Seed and Idriss [33].

2. UBC3D-PLM parameters from DMT

The UBC3D-PLM model employs two yield surfaces, the primary and secondary yield surfaces, to simulate the cyclic behaviour of sandy soils. The yield surfaces are defined by the Mohr-Coulomb yield function as follows:

$$f_m = \frac{\sigma'_{max} - \sigma'_{min}}{2} - \left(\frac{\sigma'_{max} + \sigma'_{min}}{2} + c' \cot \varphi'_{p}\right) \sin \varphi'_{m} \tag{2}$$

where σ'_{max} and σ'_{min} are the maximum and minimum principal effective stresses, respectively, c' is the cohesion of the soil, φ'_p is the peak effective friction angle of the soil and φ'_m is the mobilised friction angle during hardening.

A stress dependent non-linear rule governs the elastic behavior that occurs within the secondary yield surface. It is defined by the elastic bulk modulus, K, and the elastic shear modulus, G, which are stress dependent according to the following equations:

$$K = k_B^e p_{ref} \left(\frac{p'}{p_{ref}} \right)^{me} \tag{3}$$

$$G = k_G^e p_{ref} \left(\frac{p'}{p_{ref}} \right)^{ne} \tag{4}$$

where k_B^e and k_G^e are the bulk and the shear modulus numbers at a reference stress level p_{ref} , respectively, \mathbf{p}' is the mean effective stress and

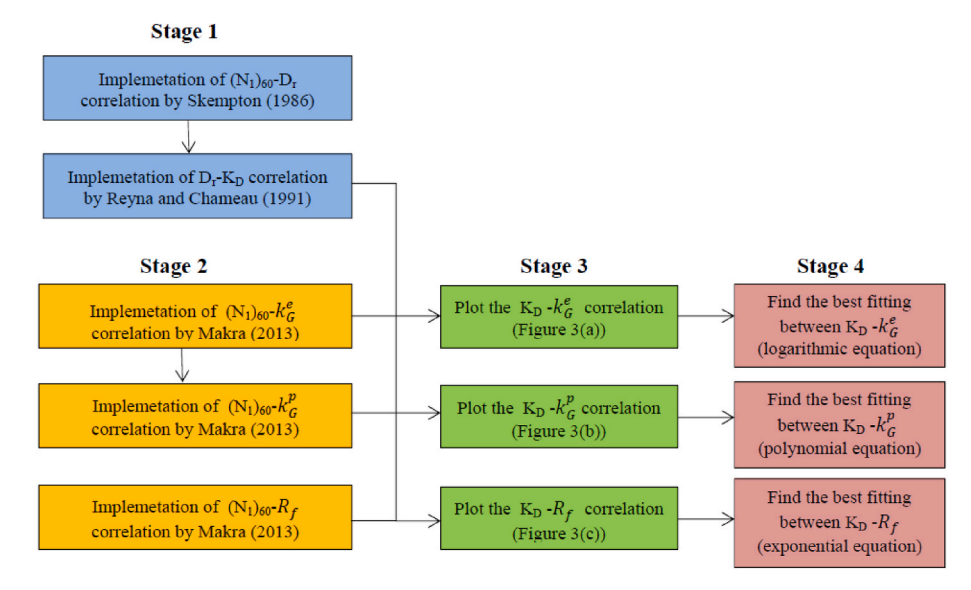


Fig. 2. Methodology for the development of the correlations between the UBC3D-PLM parameters and K_{D} .

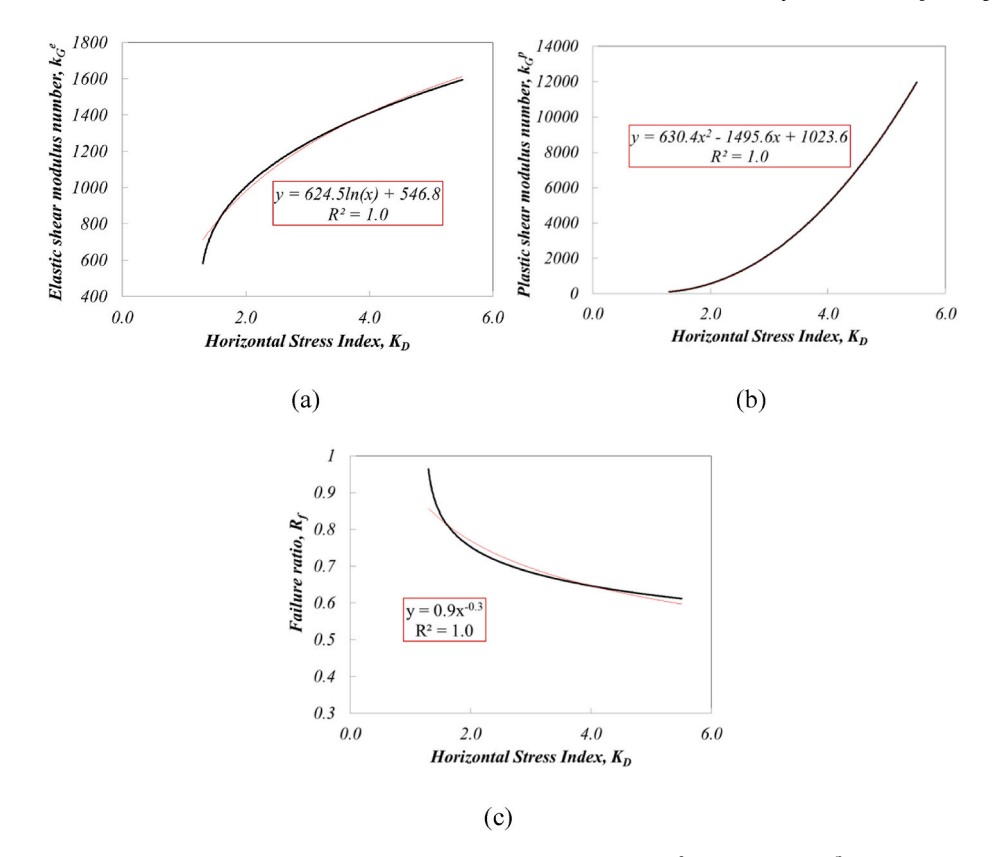


Fig. 3. Correlations for estimating the initial parameters of the UBC3D-PLM soil model: (a) k_G^e - K_D curve, (b) k_D^e - K_D curve and (c) R_f - K_D curve.

me and *ne* are two parameters that define the rate of stress dependency of stiffness.

A non-associated flow rule, based on the Drucker-Prager model, is employed in the model. Moreover, the primary yield function has an isotropic hardening rule defined by the following relation:

$$d\sin\varphi_{m}' = 1.5k_{G}^{p} \left(\frac{p'}{p_{ref}}\right)^{np} \frac{p_{ref}}{p'} \left(1 - \frac{\sin\varphi_{m}'}{\sin\varphi_{ult}'}\right)^{2} d\lambda \tag{5}$$

where k_G^P is the plastic shear modulus number, np is the plastic shear modulus exponent, $d\lambda$ is the plastic strain increment multiplier, ϕ'_{ult} is the ultimate mobilised friction angle that is derived from the failure ratio, R_f :

$$R_f = \frac{\sin \varphi_p'}{\sin \varphi'}.$$
 (6)

The secondary surface has a kinematic hardening rule. To simulate the effect of soil densification during secondary loading, the plastic shear modulus number, k_G^p , increases as a function of the number of cycles as follows:

$$k_{G,secondary}^{p} = k_{G}^{p} \left(4 + \frac{n_{rev}}{2} \right) hardf_{dens}$$
 (7)

where $k_{G,secondary}^{P}$ is the secondary plastic shear modulus number, n_{rev} is the number of shear stress reversals from loading to unloading (or vice versa), *hard* is a factor that corrects the densification rule for loose sand and f_{dens} is a user-input parameter for calibrating the densification rule.

To account for the stiffness degradation of the soil caused by the post-liquefaction behaviour in loose non-cohesive sands or cyclic mobility in dense non-cohesive sands, the plastic shear modulus, k_G^P , is gradually reduced as a function of generated plastic-deviatoric strain during soil dilatation:

$$k_{G,post-liquefaction}^{P} = k_{G}^{P} E_{dil}$$
 (8)

$$E_{dil} = max \left(e^{-110\varepsilon_{dil}}; f_{Epost} \right) \tag{9}$$

where $k_{G,post-liquefaction}^{P}$ is the plastic shear modulus number during liquefaction, ε_{dil} is the accumulation of plastic-deviatoric strain produced during dilatation of the soil element and f_{Epost} is the input parameter that limits E_{dil} [30,34,35].

The proper way to obtain parameters for the UBC3D-PLM model, as well as for most soil constitutive models for liquefaction studies, is by curve fitting from cyclic triaxial tests or cyclic direct simple shear tests [36].

However, often only data from in situ tests are available. In this regard, the CPT and the SPT are the two most employed in situ tests for evaluation the liquefaction resistance [6]. For this reason, Beaty and Byrne [37] proposed specific correlations between the model parameters and the corrected SPT blow counts, $(N_1)_{60}$, for the generic calibration of the UBCSAND model (Version 904aR). Then, Makra [38] modified these equations for the UBC3D-PLM soil model, as follows:

$$k_G^e = 21.7 \times 20(N_1)_{60}^{0.3333}$$
 (10)

$$k_B^e = 0.7k_G^e (11)$$

$$k_G^p = 0.003 k_G^e (N_1)_{60}^2 + 100 (12)$$

$$\varphi_p = \varphi_{cv} + \frac{(N_1)_{60}}{10} + \max\left(0; \frac{(N_1)_{60} - 15}{5}\right)$$
(13)

$$R_f = 1.1(N_1)_{60}^{-0.15} < 0.99 (14)$$

where φ_{cv} is the constant volume friction angle that can be obtained from SPT test in turn [39,40]. The suggested values for the index

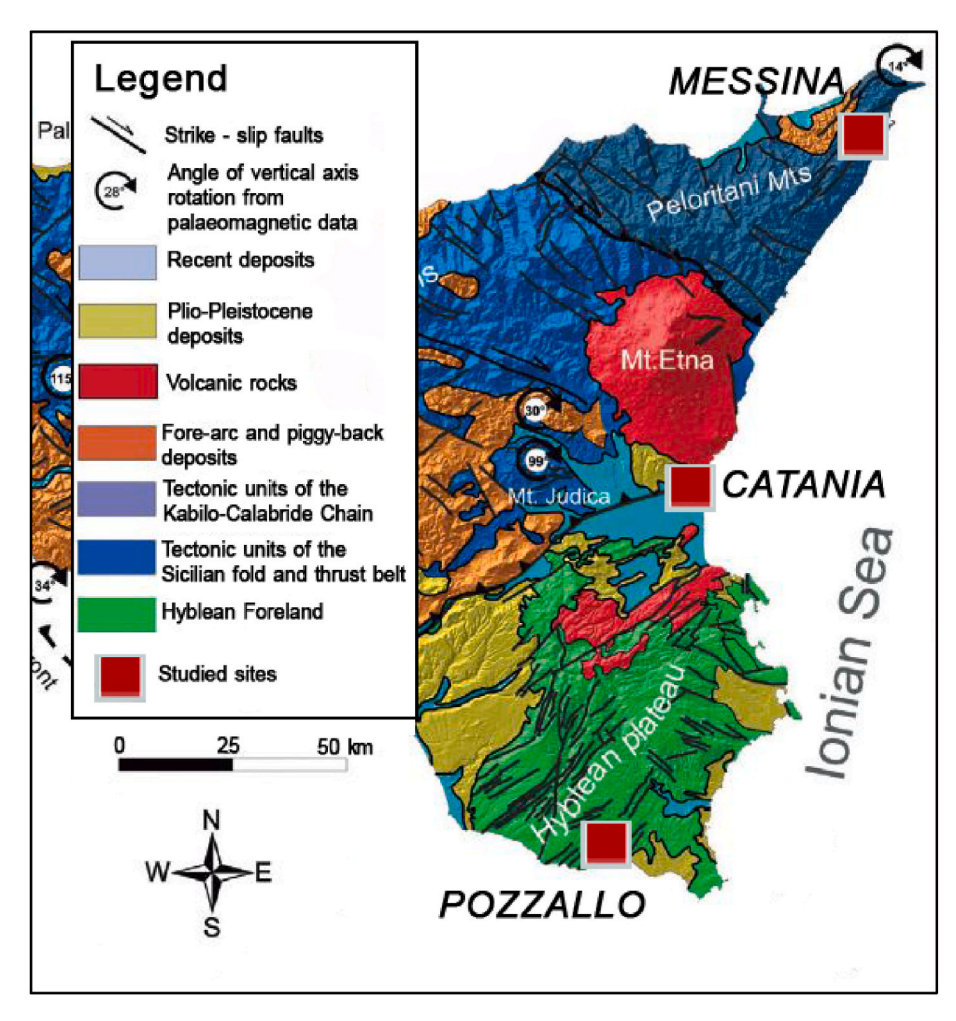


Fig. 4. Geological sketch map of eastern Sicily with the location of the studied sites (After Barreca and Monaco [48]; modified).

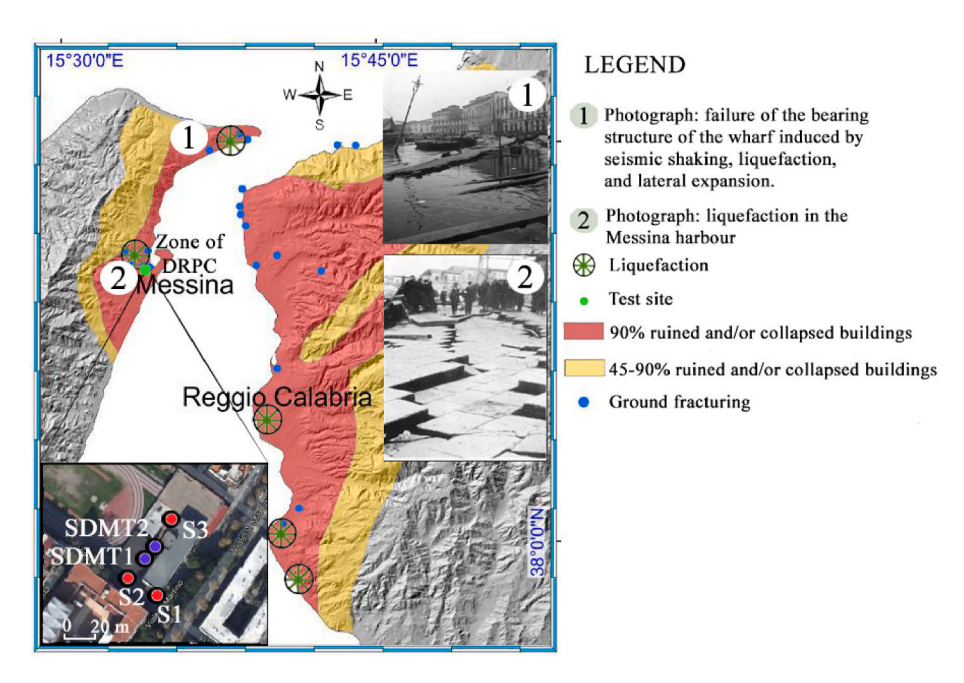


Fig. 5. Evidence of liquefaction [49,50], percentage of damaged buildings and recorded coseismic ground fracturing in Messina and Reggio Calabria cities following the 1908 earthquake (After Barreca et al. [51]; modified). Location of in situ tests in the zone of the DRPC.

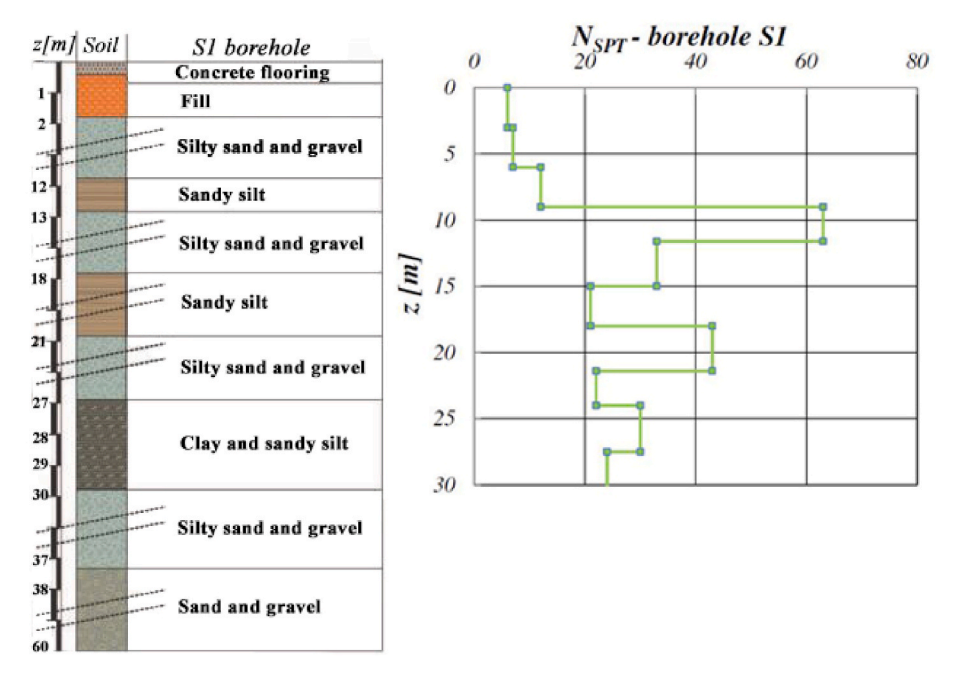


Fig. 6. Soil profile and N_{SPT} results versus depth obtained from S1 borehole.

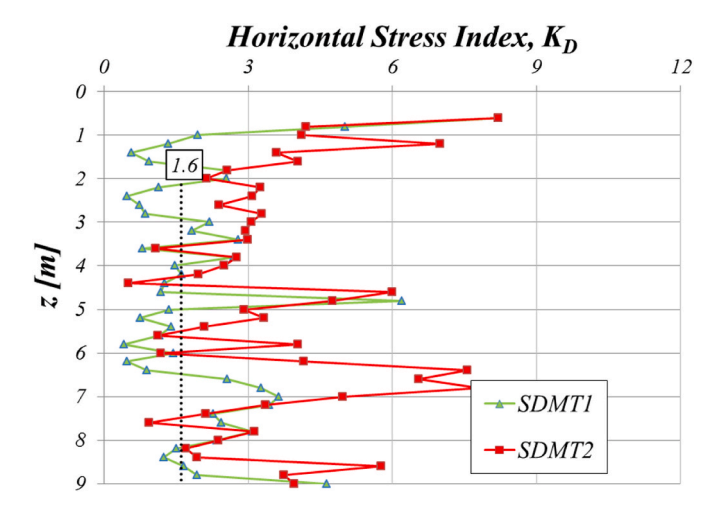


Fig. 7. Results of the SDMT1 and SDMT 2 in terms of K_D obtained at DRPC area in the city of Messina.

parameters that describe the rate of stress-dependency are me=ne=0.5 and np=0.4.

Specific correlations between the parameters of the UBC3D-PLM model and the K_D from DMT are proposed in this work. The correlations recommended by Makra [38] for SPT are translated into "equivalent" correlations for the DMT using the relative density, D_r , as intermediate parameter according to the following procedure.

- Evaluation of D_r corresponding to the values of (N₁)₆₀ using the well-known correlation proposed by Skempton [41];
- (2) Calculation of the values of K_D using the K_D - D_r correlation by Reyna and Chameau [42] reported in Fig. 1. This correlation, defined for $1.3 < k_D < 5.5$, can be approximated by the following equation:

$$K_D = 0.0007[D_r(\%)]^2 - 0.0186 D_r(\%) + 1.3939$$
 (15)

(3) Plot the correlations for the DMT derived from SPT.

Fig. 2 shows, in detail, the diagram representing the methodology steps for the development of the correlations between the model parameters and K_D . Fig. 3 reports the alternative correlations for the generic and initial calibration of the UBC3D-PLM soil model from K_D values.

The proposed correlations can be approximated by the following equations:

$$k_G^e = 624.5 \ln K_D + 546.8 \tag{16}$$

$$k_B^e = 0.7k_G^e \tag{17}$$

$$k_G^p = 630.4 K_D^2 - 1495.6 K_D + 1023.6$$
 (18)

$$R_f = 0.9 \, K_D^{-0.3} \tag{19}$$

The strength parameters can be derived directly from triaxial or direct shear simple tests, if available; otherwise, the correlations reported in TC16 DMT Report by Marchetti et al. [44] can be employed. The suggested values for the index parameters are me = ne = 0.5 and np = 0.4

In this work, the CRR curve for SPT was translated into an "equivalent" CRR curve for K_D using D_r as intermediate parameter. D_r was considered a suitable intermediary as it is one of the most important factor affecting the liquefaction resistance of soil, because of the presence in literature of well-known and widely used correlations between D_r and SPT blow counts, and the possibility of deriving K_D from D_r using the correlation by Reyna and Chameau [42].

Therefore, it is important to highlight that the liquefaction triggering curve was not developed directly from DMT datapoints but using an indirect correlation with the relative density from SPT case histories. Despite the fact that the equation is verified for CRR- K_D datapoints obtained after the Loma Prieta 1989 earthquake in the San Francisco Bay (Section 4), this interpretation could be significantly improved considering directly DMT data. However, the approach used in this study was adopted for two main reasons. The first is the extensive and decadeslong experience that led to the current procedure for evaluating CRR from SPT. Moreover, another important reason is given by the large number of SPT case histories [6], which have continued to increase with recent earthquakes (e.g the 2010–2011 Canterbury seismic sequence in New Zealand and the 2011 Tohoku earthquake in Japan), compared to

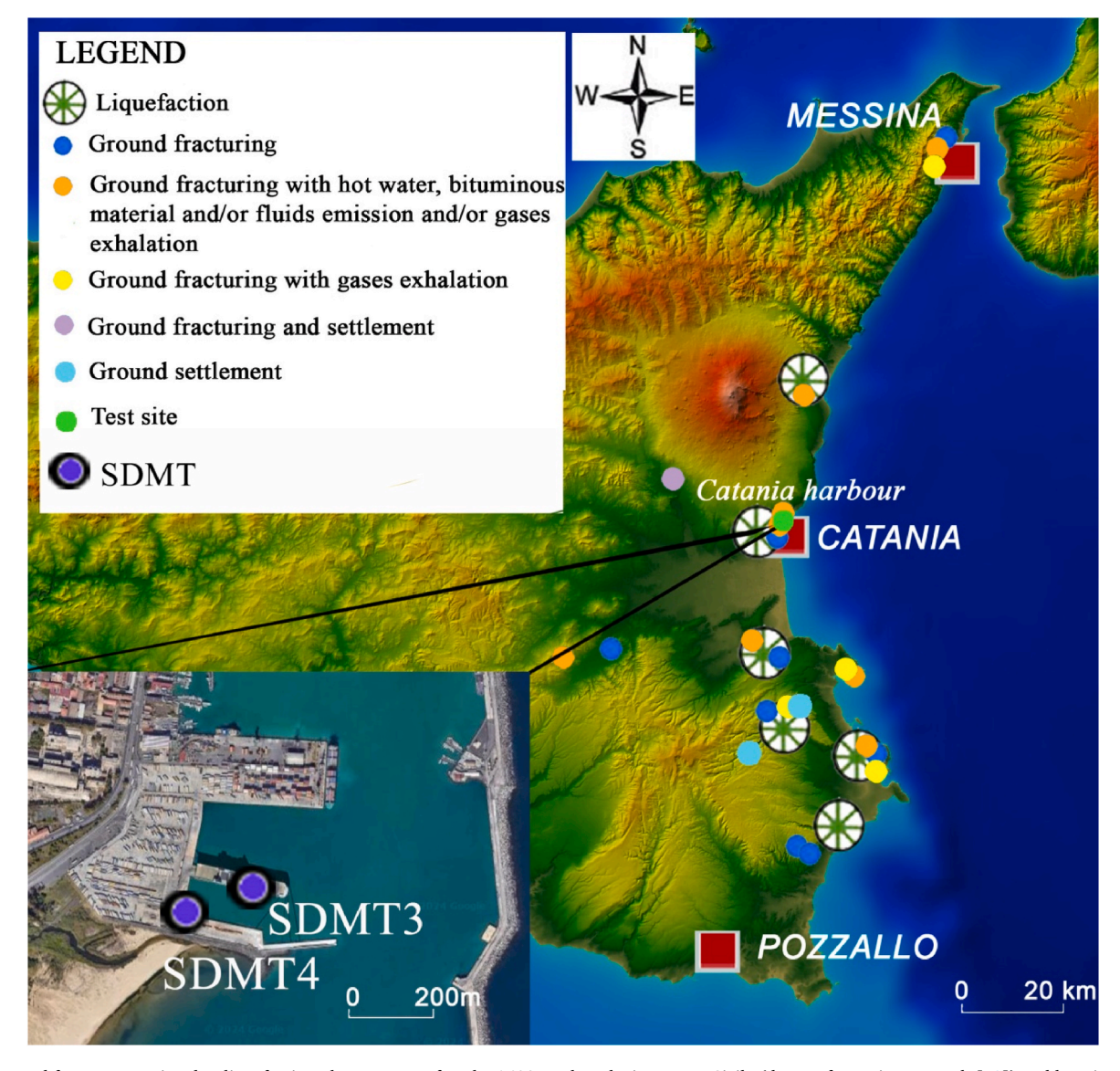


Fig. 8. Ground features associated to liquefaction phenomenon after the 1693 earthquake in eastern Sicily (dataset from Pirrotta et al. [50]) and location of SDMTs in Catania harbour. Basemap from Tarquini et al. [53].

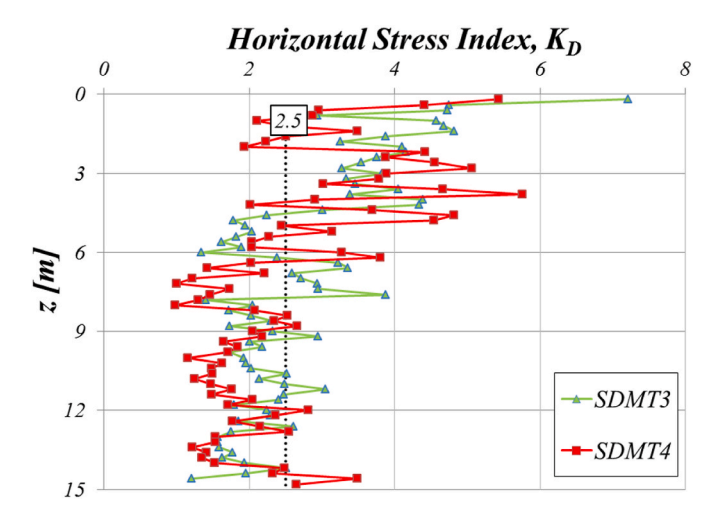


Fig. 9. Results of the SDMT3 and SDMT4 in terms of K_D in the Catania harbour.

DMT data.

The developed equations were employed for calibrating the UBC3D-PLM model from DMT data to simulate the behaviour of liquefiable soils at various sites in eastern Sicily (Italy), which experienced numerous major earthquakes with liquefaction phenomenon observed in history. This case study can be served as validation for the developed equations as it demonstrates the wide applicability of the correlations at different $K_{\rm D}$ values characteristic of the appropriately chosen sites (Section 3). The cyclic strength curve was reproduced by simulating CDSS in PLAXIS, showing a satisfactory fit between the calibrated model and the liquefaction triggering curve for each test site.

The eastern part of Sicily is considered as one of the most seismically active areas in Italy characterized by a high level of crustal activity, which is the cause of large seismic events (1169, 1693, 1783, 1818, 1908, 1990) [45–47]. In this work, the new proposed correlations were employed for the initial and generic calibration of the UBC3D-PLM model, implemented in the finite element code PLAXIS (Bentley), to

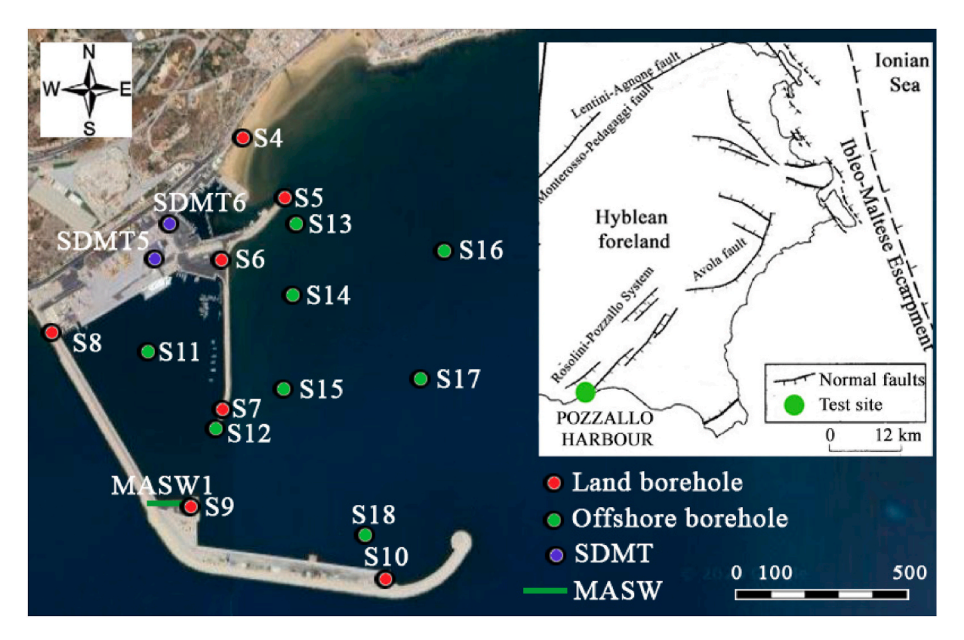


Fig. 10. Structural map of southeastern Sicily (After Giampiccolo et al. [54]; modified) and plan view of Pozzallo harbour with the location of in situ tests.

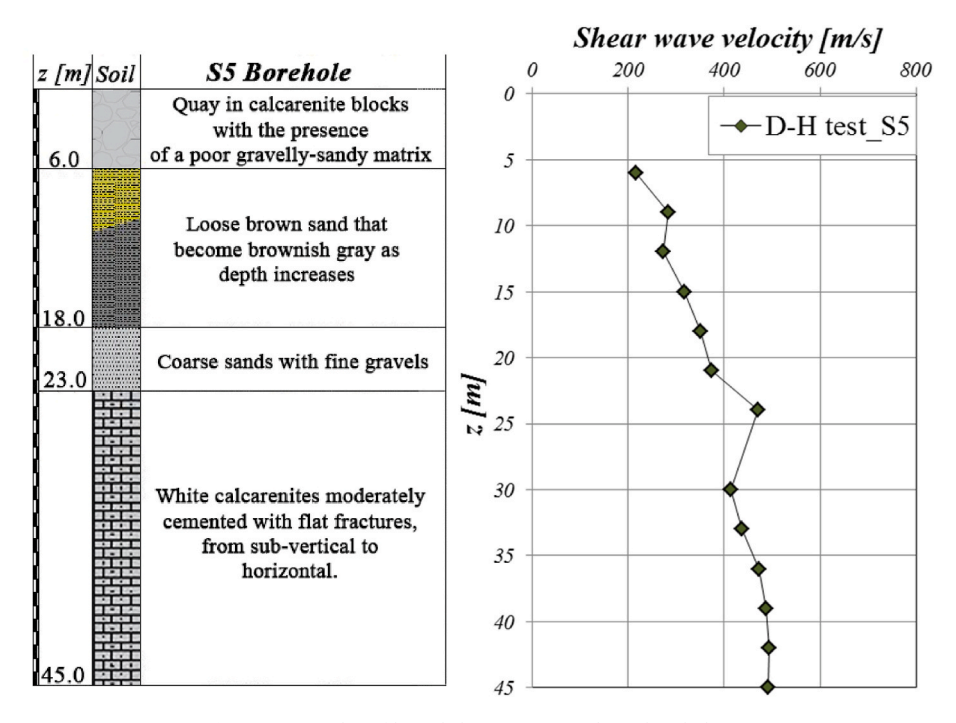


Fig. 11. (a) Soil profile and (b) D-H test results in borehole S5.

simulate the behavior of liquefiable sites located in the cities of Messina, Catania and Pozzallo (Sicily, Italy) (Fig. 4).

3.1. Zone of the Regional Civil Defence Department (DRPC) in the city of Messina

On 28th December 1908, one of the most strongest seismic events that affected Italy during historical time (Intensity MCS XI, Mw = 7.24) hit the cities of Messina and Reggio Calabria. Evidence of liquefaction, such as water from the ground, mud or sand boils, were observed in the areas of Messina and Reggio Calabria. Ground fracturing was also reported in several localities [49] (Fig. 5).

The zone of the Regional Civil Defence Department (DRPC) in the city of Messina was chosen as test site. Several laboratory and in situ

tests, which locations are reported in Fig. 5, were performed in the zone of the DRPC, including n. 3 boreholes (S1, S2 and S3), n. 2 Standard Penetration Tests (SPT), n. 1 Down-Hole (D-H) test, n. 1 Cross-Hole (C-H) test, n. 2 Seismic Dilatometer Marchetti Tests (SDMT), n. 6 Direct Shear Tests (DST), n. 2 Consolidated Undrained Triaxial Tests (CUTXT), n. 4 Cyclic Loading Torsional Shear Tests (CLTST) and n. 4 Resonant Column Tests (RCT) [52].

Fig. 6 presents the soil profile and the SPT results for the S1 borehole, as an example. Based on the results, it is possible to observe that the zone of the DRPC mainly consists of silty sand and gravel with horizons of clay and sandy silt. The water table lies around 3 m below the ground surface. SDMT1 is limited in depth to 9.0 m because the inclinometers signaled a variation of the verticality exceeding the permitted limit at greater depths. Therefore, the test was repeated in the immediate

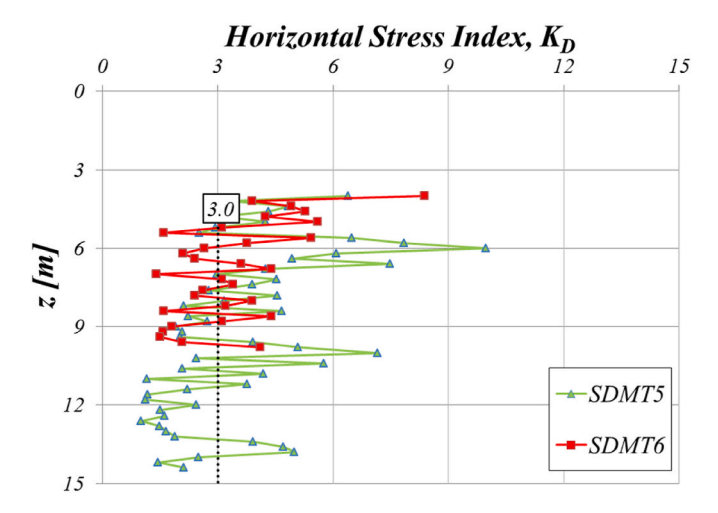


Fig. 12. Results of the SDMT5 and SDMT 6 in terms of $K_{\rm D}$ obtained at Pozzallo harbour.

vicinity. The depth of 32 m was reached for the SDMT2. The K_D variation until 9 m, obtained from SDMT1 and SDMT2, is displayed in Fig. 7.

3.2. Catania harbour

On 11th January 1693, the Val di Noto earthquake (Intensity MCS X-XI, Mw = 7.32), that is one of the largest seismic event in Italy with the 1908 Messina earthquake, caused the destruction of 57 cities and 60,000 casualties. Fig. 8 reports the sites where geological evidence of lique-faction (e.g. sand boils, sand hills and sand/mud volcano), correlated to the 1693 earthquake, were found. Ground deformations are also showed

The Catania harbour was chosen as test site. Evidence of liquefaction and ground fracturing were found near this area after the 1693 earth-quake (Fig. 8). An investigation campaign was performed to evaluate the geotechnical characteristics of the sandy soil including n. 3 DST, n. 3 Triaxial Consolidated Drained (CD) Tests, n. 6 RCT and n. 2 SDMT, which locations are reported in Fig. 8. The Catania harbour site mainly consists of fine sands with thin limestones. The groundwater level was measured at around 1 m below ground level. The results of the SDMT3 and SDMT4 in terms of horizontal stress index, K_D , are reported in Fig. 9.

3.3. Pozzallo harbour

The city of Pozzallo, located on the south-eastern coast of Sicily, is part of the Hyblean Plateau (Fig. 4), which represents a contact area between the Eurasian and African regions. The strongest seismic events

in Southeastern Sicily are generated by the offshore NNW-SSE-trending fault system, while the weakest earthquakes are linked to secondary internal faults (e.g. the Rosolini-Pozzallo-Ispica fault system) [54] (Fig. 10).

An extensive investigation campaign was carried out at Pozzallo harbour that is one of the most important ports in Sicily. Among in situ tests, boreholes, SPT tests, SDMTs, D-H tests and a Multichannel Analysis Surface Waves (MASW) were performed (Fig. 10). Moreover, n. 26 undisturbed and n. 8 disturbed samples were retrieved from land boreholes to be analyzed by standard laboratory tests, including DST.

Results of boreholes indicate a 5–6 m thick layer of calcarenite blocks overlaying brown-grey loose sand to a depth of about 18 m and the presence of coarse sands with fine gravels from $\sim\!18$ m to $\sim\!23$ m on moderately cemented calcarenites. The water table lies around 1 m below the ground surface. The soil stratigraphy and the V_S profile obtained from the S5 borehole are reported in Fig. 11. Values of K_D versus depth obtained from SDMT5 and SDMT 6 are showed in Fig. 12.

4. Calibration of the UBC3D-PLM model

For the generic calibration of the UBC3D-PLM model, the parameters were estimated from the K_D using Equations (16)–(19) proposed in this study.

With reference to the DRPC area in the city of Messina, the fill layer (from 0 to 2 m) was not considered liquefiable as the groundwater level was at the depth of 3 m. Instead, the slightly silty sand and gravel layer (from 2 to 9 m) was modelled with $\rm K_D=1.6$ (Fig. 7). This value is closer to the results obtained by SDMT1 from 2 to 9 m and is consistent with the corrected SPT value (Fig. 6), evaluated in accordance with the procedure proposed by Idriss and Boulanger [55], equal to 7.35. Indeed, using the relative density, $\rm D_r$, as intermediate parameter, the following relationship that relates the $\rm K_D$ and the corrected SPT value was obtained:

Table 1Testing conditions for each test site used in PLAXIS for the simulation of the CDSS tests.

Conditions	DRPC area	Catania harbour	Pozzallo harbour	
Type of test	Undrained	Undrained	Undrained	
K_0 -value	0.5	0.5	0.5	
$ \sigma_{yy} $	100 kN/m^2	100 kN/m^2	100 kN/m^2	
Test control	Stress	Stress	Stress	
$ au_{xy}$	$10kN/m^2$	19 kN/m^2	26 kN/m^2	

where K_0 -value is the ratio of lateral stress over axial stress; $|\sigma_{yy}|$ is the absolute value of the initial vertical shear at which the sample is consolidated; τ_{xy} is the applied shear stress amplitude.

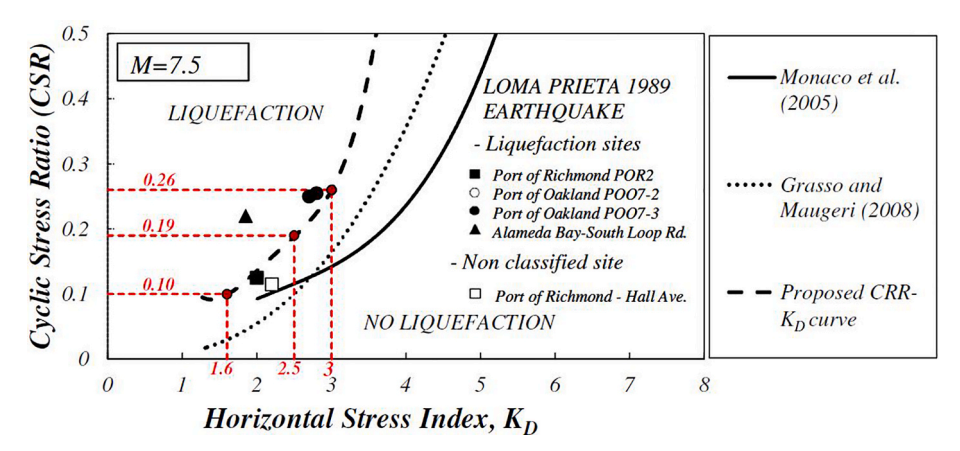


Fig. 13. Comparison of "equivalent" DMT-based liquefaction triggering curves and Loma Prieta 1989 earthquake datapoints by Mitchell et al. [56].

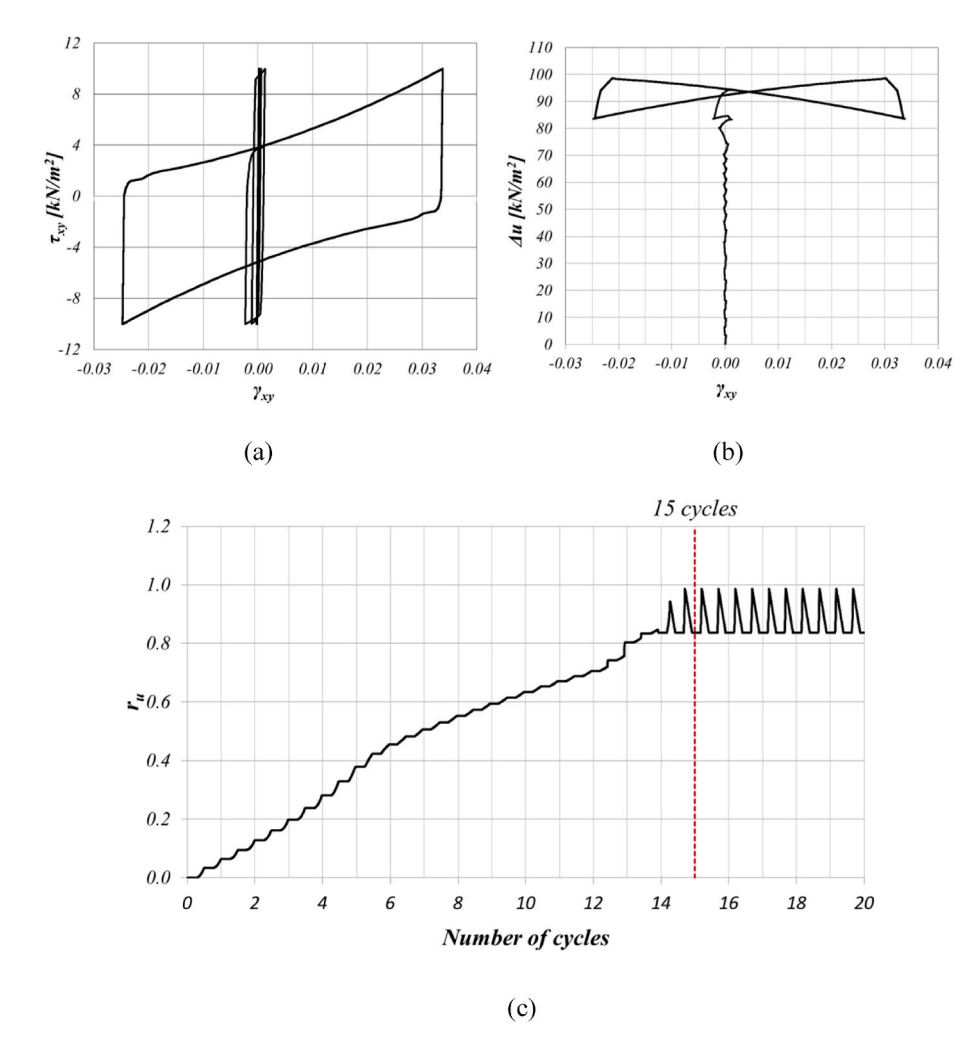


Fig. 14. CDSS test results obtained for the CSR = 0.10 (DRPC area): (a) shear stress (τ_{xy}) versus shear strain (γ_{xy}) , (b) excess water pore pressure (Δu) versus shear strain (γ_{xy}) and (c) excess pore water pressure ratio (r_u) against the numbers of cycles.

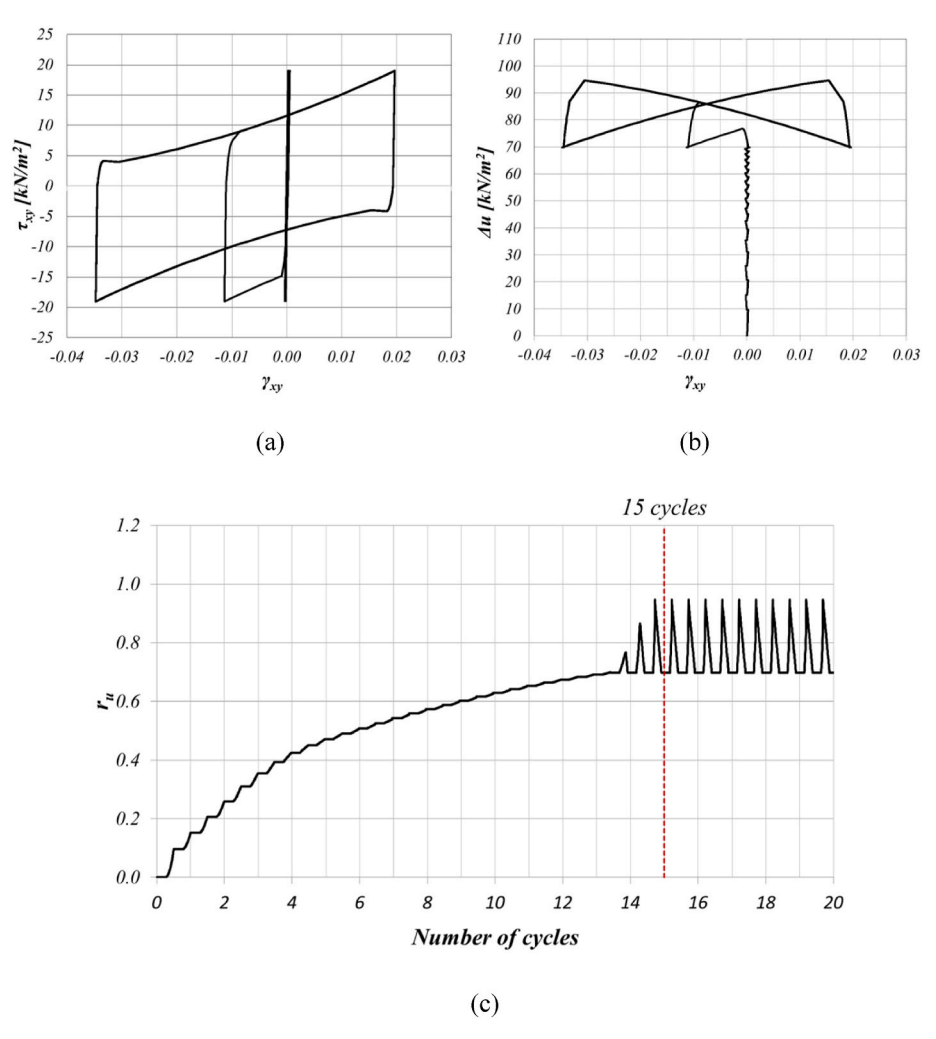


Fig. 15. CDSS test results obtained for the CSR = 0.19 (Catania harbour): (a) shear stress (τ_{xy}) versus shear strain (γ_{xy}) , (b) excess water pore pressure (Δu) versus shear strain (γ_{xy}) and (c) excess pore water pressure ratio (r_u) against the numbers of cycles.

$$K_D = 0.0002 (N_1)_{60cs}^2 + 0.0804 (N_1)_{60cs} + 0.9772$$
 (20)

The strength parameters were derived from the DSS test carried out on a sample taken in S1 borehole at a depth of 7.0–7.4 m.

In relation to the Catania harbour, the sandy layer (from 2 to 15 m) was modelled with $K_D=2.5$ (Fig. 9), corresponding to a corrected SPT value of 18 obtained by using Equation (20), considering the dominant liquefaction effects up to a depth of 15 m. Moreover, DST and Triaxial tests show that the investigated soil is cohesionless and with a shear resistance value of about 37° . Finally, with reference to the Pozzallo harbour, the first 5 m (quay in calcarenite blocks) were not considered liquefiable. Instead, the brown-grey sand layer (from 5 to 15 m) was modelled with $K_D=3.0$ (Fig. 12) corresponding to a corrected SPT value of 24 obtained using Equation (20). The strength parameters were derived from the DST tests carried out on samples taken at a depth of 5.0 m–15.0 m.

In this work, the CRR curve for SPT [6], presented in Equation (21), is translated into an "equivalent" CRR curve for K_D using D_r as intermediate parameter. In Fig. 13, the CRR- K_D curve, approximated by Equation (22), is compared to the relationships proposed previously by Monaco et al. [17] and Grasso and Maugeri [18]. Equation (21) was derived including additional case histories in the liquefaction triggering database (e.g. 2010–2011 Canterbury earthquake sequence in New Zealand and the 2011 Toholu earthquake in Japan). Moreover, liquefaction datapoints, identified at various locations by Mitchell et al. [56] after the Loma Prieta 1989 earthquake in San Francisco Bay region, are

also reported in Fig. 13. As can be seen from the chart, the relationship proposed here provides higher values of CRR.

$$\textit{CRR} = exp \left\{ \frac{(N_1)_{60cs}}{14.1} + \left(\frac{(N_1)_{60cs}}{126} \right)^2 - \left(\frac{(N_1)_{60cs}}{23.6} \right)^3 + \left(\frac{(N_1)_{60cs}}{25.4} \right)^4 - 2.8 \right\} \tag{21}$$

$$CRR = 0.054 K_D^4 - 0.475 K_D^3 + 1.563 K_D^2 - 2.172 K_D + 1.166$$
 (22)

The model was calibrated to the proposed CRR- K_D curve (Equation (22)) using two fitting parameters: the densification factor, f_{dens} , and the post-liquefaction factor, f_{Epost} [30]. These fitting parameters were derived from the simulation of cyclic direct simple shear tests (CDSS), whose conditions are showed in Table 1 for each test site, using PLAXIS software. The sample was considered liquefied when the single amplitude of shear strain exceed 3 % [57].

According to the proposed CRR- K_D curve (Fig. 13), values of $CSR_M = 7.5$, $\sigma'=1$ atm of 0.10, 0.19 and 0.26 were derived at K_D of 1.6, 2.5 and 3.0 for the DRPC area, the Catania harbour and the Pozzallo harbour, respectively. Moreover, based on the relationship proposed by Idriss and Boulanger [57], an earthquake of $M_W = 7.5$ coincides with a number of equivalent stress cycles of 15. Hence, the values of the fitting parameters, f_{dens} and f_{Epost} , were obtained when liquefaction was reached for a number of cycles of 15 applying a CSR of 0.10, 0.19 and 0.26 for the DRPC area, the Catania harbour and the Pozzallo harbour, respectively.

CDSS test results obtained for the CSR of 0.10 (DRPC area), 0.19 (Catania harbour) and 0.26 (Pozzallo harbour) are displayed in

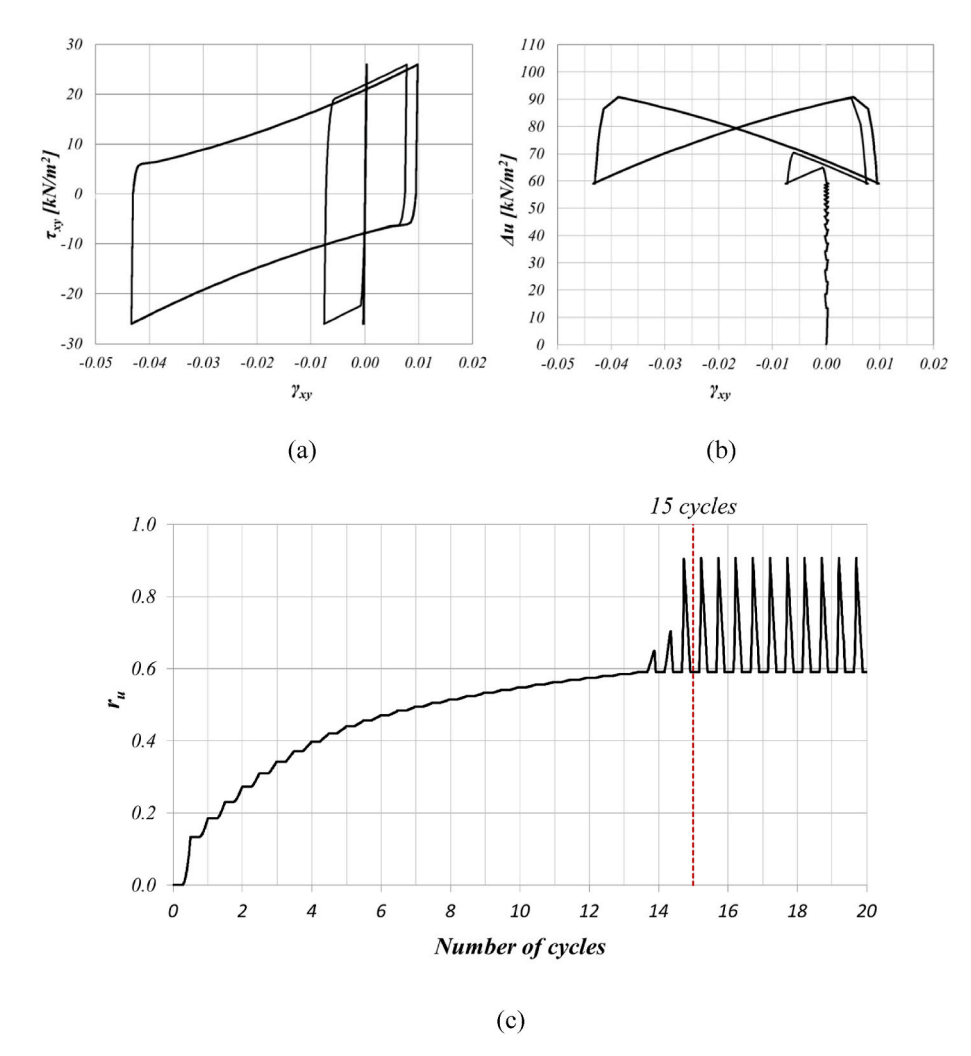
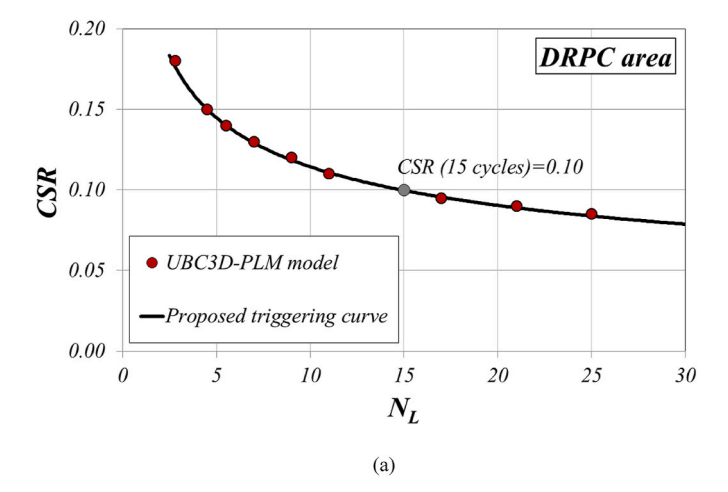
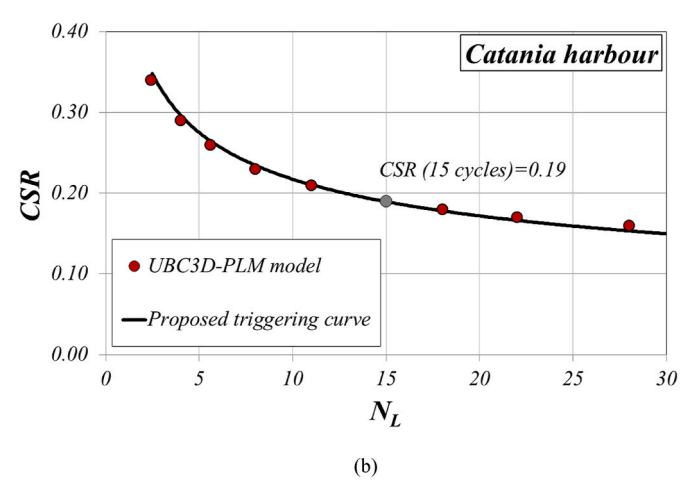


Fig. 16. CDSS test results obtained for the CSR = 0.26 (Pozzallo harbour): (a) shear stress (τ_{xy}) versus shear strain (γ_{xy}) , (b) excess water pore pressure (Δu) versus shear strain (γ_{xy}) and (c) excess pore water pressure ratio (r_u) against the numbers of cycles.





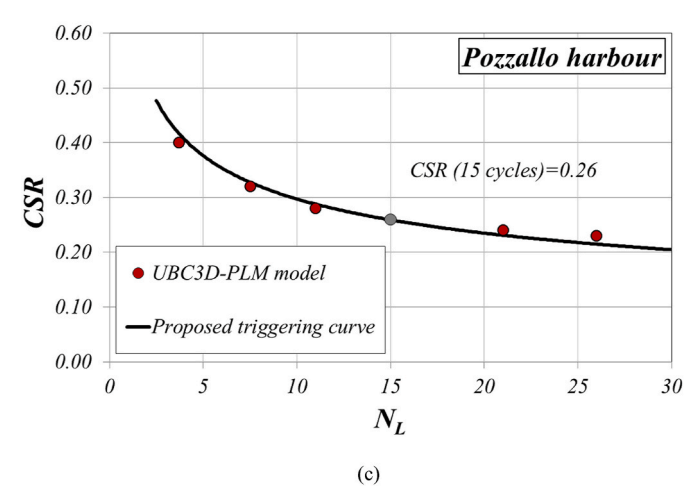


Fig. 17. Comparison between the calibrated UBC3D-PLM model and the proposed triggering curve from Dilatometer Marchetti Test (DMT) for: (a) the DRPC area, (b) the Catania harbour and (c) the Pozzallo harbour.

Figs. 14–16, respectively, in terms of shear stress, τ_{xy} , and excess water pore pressure, Δu , versus shear strain, γ_{xy} , and excess pore water pressure ratio, r_u , against numbers of cycles.

Additional CDSS tests were simulated for each test site by modifying the applied CSR. Fig. 17 reports the CSR versus the equivalent number of cycles needed for the liquefaction onset, N_L , obtained from PLAXIS for the DRPC area (Fig. 17(a)), the Catania harbour (Fig. 17(b)) and the Pozzallo harbour (Fig. 17(c)). In order to obtain the CSR- N_L curve, the magnitude scaling factor (MSF) [57] was employed to adjust the

Table 2Parameters of the UBC3D-PLM model for liquefiable sandy soils at the DRPC area in the city of Messina, the Catania harbour and the Pozzallo harbour.

Parameter	Symbol	Unit	DRPC area	Catania harbour	Pozzallo harbour
Saturated unit weight of soil	γsat	kN/ m ³	18.34	17.30	17.00
Peak friction angle	φ'_{p}	0	34	37	38
Constant volume friction angle	ϕ'_{cv}	0	33	36	37
Cohesion	c'	kN/ m ²	1	1	1
Elastic bulk modulus factor	k_{B}^{e}	-	623	807	885
Elastic shear modulus factor	k_{G}^{e}	-	890	1152	1264
Plastic shear modulus factor	kg	-	270	1196	2239
Rate of stress- dependency of elastic bulk modulus	me	-	0.5	0.5	0.5
Rate of stress- dependency of elastic shear modulus	ne	-	0.5	0.5	0.5
Rate of stress- dependency of plastic shear modulus	np	-	0.4	0.4	0.4
Failure ratio	R_f	-	0.80	0.72	0.69
Reference pressure	ра	kN/ m ²	100	100	100
Densification factor	f_{dens}	_	0.76	0.60	0.74
Post-liquefaction factor	f_{Epost}	_	0.20	0.15	0.10
Horizontal stress index	K_D	-	1.60	2.5	3.0

induced CSR for an earthquake of magnitude M to an equivalent CSR for a reference magnitude of 7.5:

$$MSF = 6.9 \exp\left(\frac{-M}{4}\right) - 0.058 \le 1.8$$
 (23)

The comparison between the calibrated UBC3D-PLM model and the proposed triggering curve, displayed in Fig. 17, shows satisfactory fit for each test site. Table 2 presents the parameters for the UBC3D-PLM model obtained using the new parameter selection procedure for the DRPC area, the Catania harbour and the Pozzallo harbour.

5. Validation of the UBC3D-PLM model from CDSS tests

In this study, CDSS tests were performed to validate the calibrated UBC3D-PLM model. The CDSS device, employed in this work, is an advanced apparatus manufactured by Controls Group (https://controlsgroup.com/product/cyclic-simple-shear-apparatus-controls/) designed to allow a sample to be consolidated and then sheared under constant volume conditions simulating an undrained shear of a saturated specimen. The CDSS device at the Soil Dynamics and Geotechnical Engineering Laboratory of the "Kore" University of Enna is showed in Fig. 18. The apparatus includes a control and data acquisition system with two 5 kN actuators that have internal displacement transducers. The standard sample has a diameter of 70 mm and a height of 20 mm. It is positioned on a pedestal and restrained by a rubber membrane and a series of slip rings.

The CDSS tests were conducted to reproduce the testing conditions used in PLAXIS for the simulation of the CDSS tests. Despite the great complexity involved in simulating the onset of liquefaction within the context of classical plasticity [58], the numerical modelling results are quite in agreement with the experimental data.

With reference to the Pozzallo case study, as an example, Fig. 19 reports the results obtained for a sandy sample retrieved from 7.50 m to 7.95 m in S5 borehole. The CDSS test was conducted on a medium-loose sample with a relative density of about 60 %. This is consistent with the



Fig. 18. Equipment at the Soil Dynamics and Geotechnical Engineering Laboratory of the "Kore" University of Enna used for CDSS tests.

value of D_r , derived from the K_D - D_r correlation by Reyna and Chameau [42], for a $K_D=3.0$ obtained at Pozzallo harbour (Fig. 12). The remoulding of the soil sample was carried out by the moist tamping with a water content of 10 % to facilitate compaction. The remoulded sample was consolidated under an effective vertical stress, $\sigma'_{\nu 0}$, of 100 kPa. The cyclic shearing was applied using sine waves with amplitudes equal to the cyclic shear stress, $\pm \tau_{cyc}$, of 26 kN/m² and a frequency of 0.1 Hz. The height of the samples was kept constant during the shearing process using the active height control. In CDSS, the CSR is defined as:

$$CSR = \frac{\tau_{cyc}}{\sigma'_{v0}} \tag{24}$$

Therefore, the applied value of CSR for this sample is equal to 0.26, reproducing the testing conditions presented in Table 1 for the Pozzallo harbour.

Fig. 19 shows the results of CDSS test in terms of hysteresis loop (Fig. 19(a)), shear strain and excess pore water pressure ratio against the numbers of cycles (Fig. 19(b) and (c)). It is possible to notice that for a number of cycles of 15 the single amplitude of shear strain is about 3 %, after which the liquefaction onset ensued with large shear strains. Even if the excess pore water pressure ratio achieves only a value of about 0.6 for a number of cycles of 15 [59,60], the comparison between the experimental and numerical results in term of $r_{\rm u}$, reported in Fig. 20, shows a similar trend.

In the hysteresis loops (Figs. 16(a) and 19(a)), there are some differences between the CDSS test and the numerical simulation. Indeed, the UBC3D-PLM model shows stiffer initial response than the experimental results. Moreover, the other significant difference is the post-liquefaction stress strain response. In order to capture the softening that occurs after the peak yield surface is reached, the post-liquefaction factor, f_{Epost} , is implemented in the UBC3D-PLM model. This factor defines the minimum shear stiffness of the soil according to Equation (9). After the peak yield surface is reached, the shear modulus is reduced in each loading cycle until it reaches the minimum value and the same loop is continuously repeated in the model. Therefore, the strains generated by the model following liquefaction are limited, even though the cyclic resistance is well predicted.

6. Conclusions

This paper presents the first attempt to provide alternative correlations for the generic and initial calibration of the UBC3D-PLM soil model from the horizontal stress index, K_D , obtained by flat dilatometer test (DMT). Many researchers suggested the DMT as an alternative in situ test to evaluate the liquefaction resistance of sands, usually estimated by SPT or CPT. Although it is not possible to separate each contribution, K_D is sensitive to several factors that affect the liquefaction resistance, such as the relative density, the stress history, the cementation and the aging.

In this study, the correlations proposed by Makra [38] for the generic and initial calibration of the UBC3D-PLM soil model from the corrected SPT blow counts are translated into "equivalent" correlations from K_D using the relative density, D_r , as intermediate parameter. As pointed out by Monaco et al. [17], this interpretation could be improved using the in situ state parameter, ξ_0 , as intermediate parameter, since the estimation of D_r from SPT is affected by some uncertainties. However, the correlation K_D - ξ_0 is not sufficiently well-defined at present. Therefore, the equations proposed in this study can be considered adequate as a first approach for the calibration of the UBC3D-PLM soil model.

These new correlations were employed to simulate the behavior of liquefiable soils of three different testing locations in eastern Sicily (Italy): the zone of the Regional Civil Defence Department (DRPC) in the city of Messina, the Catania harbour and the Pozzallo harbour. Laboratory and in situ tests, among them SDMTs, were conducted for each test site.

For the generic and initial calibration of the UBC3D-PLM model for each test site, the input parameters were obtained from $K_{\rm D}$ values using the equations proposed in this study. Then, the model was calibrated to the proposed CRR- $K_{\rm D}$ curve using the fitting parameters $f_{\rm dens}$ and $f_{\rm Epost}$ by the simulation of cyclic direct simple shear tests (CDSS) in PLAXIS software.

The CRR curve for SPT [6] was translated into an "equivalent" CRR curve for K_D using D_r as intermediate parameter. To demonstrate the reliability of the proposed approach for simulating liquefaction resistance and potentials, the cyclic strength curve, which relates the cyclic resistance with the K_D values, was reproduced in PLAXIS using the suggested correlations. CDSS tests were simulated for different values of

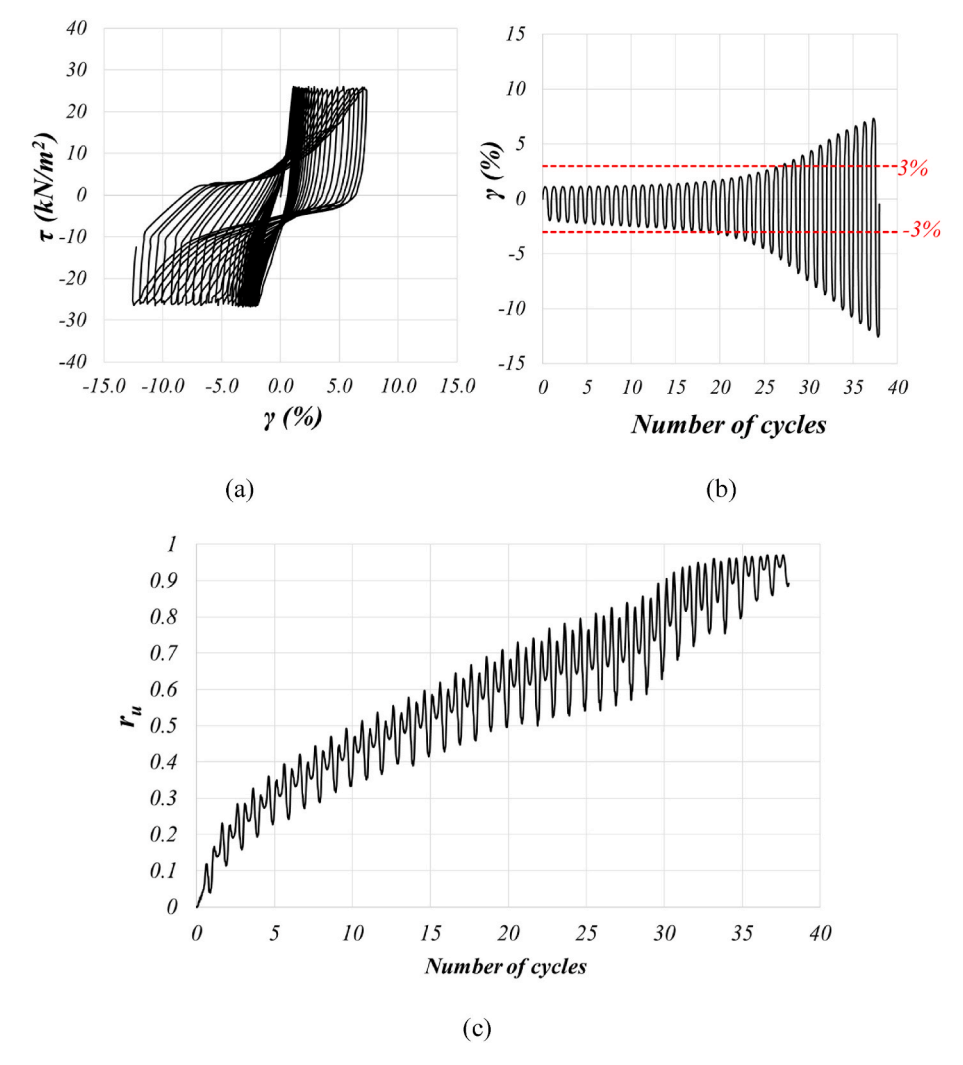


Fig. 19. Experimental results obtained from CDSS testing (CSR = 0.26): (a) shear stress (τ_{xy}) versus shear strain (γ_{xy}), (b) shear strain (γ_{xy}) and (c) excess pore water pressure ratio (τ_{xy}) against the numbers of cycles.

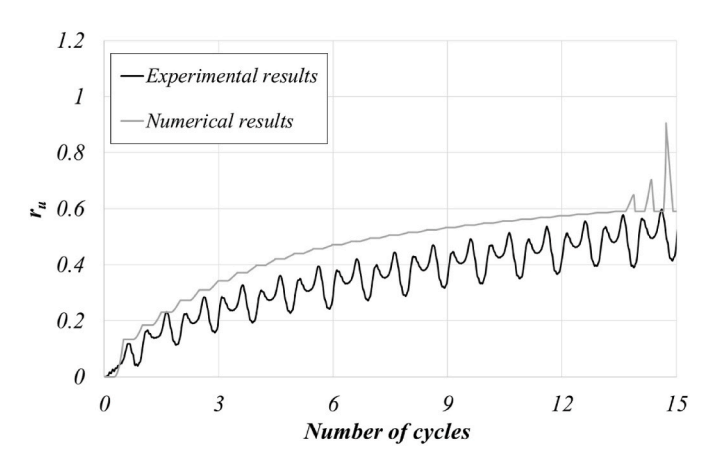


Fig. 20. Comparison between the experimental and numerical results in term of excess pore water pressure ratio against the numbers of cycles.

the CSR. The comparison between the proposed correlation and the calibrated UBC3D-PLM model shows a satisfactory convergence for each test site. In view of this parametrical fitting, this work provides valuable alternative correlations for the generic and initial calibration of the UBC3D-PLM soil model from the horizontal stress index, K_D , and

important information for the future assessment of soil liquefaction and its effects on structures in the investigated areas characterized by medium-high seismic risk. Finally, in order to evaluate the performance of the suggested calibration and validate the applicability of the proposed procedure, CDSS tests were also carried out using the apparatus available at the Soil Dynamics and Geotechnical Engineering Laboratory of the University Kore of Enna (Italy). The CDSS tests were performed to reproduce the testing conditions employed in PLAXIS for the calibration of the UBC3D-PLM soil model. The results reported in this work for the Pozzallo harbour, as an example, show that the numerical results are in close agreement with the experimental data. Indeed, despite some limitations of the model in predicting the stress-strain behaviour, a satisfactory match between the numerical simulation and the CDSS test was achieve, especially for the determination of the liquefaction onset.

CRediT authorship contribution statement

F. Castelli: Writing – review & editing, Supervision, Methodology, Conceptualization. **S. Grasso:** Writing – review & editing, Writing – original draft, Methodology, Formal analysis, Conceptualization. **V. Lentini:** Writing – review & editing, Supervision, Methodology, Conceptualization. **M.S.V. Sammito:** Writing – review & editing, Writing – original draft, Software, Methodology, Formal analysis, Conceptualization.

Declaration of competing interest

The authors declare that they have no known competing financial interests or personal relationships that could have appeared to influence the work reported in this paper.

Data availability

The data that has been used is confidential.

Acknowledgements

The authors wish to thank the editor and all anonymous reviewers for their valuable comments and suggestions.

This study was carried out within the RETURN Extended Partnership and received funding from the European Union Next-GenerationEU (National Recovery and Resilience Plan – NRRP, Mission 4, Component 2, Investment 1.3 – D.D. 1243 2/8/2022, PE0000005).

References

- Castelli F, Cavallaro A, Grasso S, Lentini V. Undrained cyclic laboratory behavior of sandy soils. Geosciences 2019:9:512.
- [2] Grasso S, Lentini V, Sammito MSV. A new biaxial laminar shear box for 1g shaking table tests on liquefiable soils. In: Proc., 4th international conference on performance based design in earthquake geotechnical engineering, Beijing, China; 2022. https://doi.org/10.1007/978-3-031-11898-2_132.
- Maugeri M, Grasso S. Liquefaction potential evaluation at Catania harbour (Italy).
 WIT Trans Built Environ 2013;1:69–81. https://doi.org/10.2495/ERES130061.
- [4] Castelli F, Grasso S, Lentini V, Massimino MR. In situ measurements for evaluating liquefaction potential under cyclic loading. In: Proc., 1st IMEKO TC4 international workshop on metrology for geotechnics; 2016. p. 79–84. Benevento, Italy.
- [5] Ashford S, Rollins K, Lane J. Blast-induced liquefaction for full-scale foundation testing. J Geotech Geoenvironmental Eng 2004;130:798–806.
- [6] Boulanger RW, Idriss IM. CPT and SPT based liquefaction triggering procedures. Center for geotechnical modeling, department of Civil and environmental engineering, college of engineering. Davis, CA, USA: University of California; 2014. Report No. UCD/CGM-14/01.
- [7] Cavallaro A, Capilleri PP, Grasso S. Site characterization by dynamic in situ and laboratory tests for liquefaction potential evaluation during Emilia Romagna earthquake. Geosciences 2018;8:242. https://doi.org/10.3390/ geosciences8070242.
- [8] Bhatnagar S, Kumari S, Sawant VA. Numerical analysis of earth embankment resting on liquefiable soil and remedial measures. Int J GeoMech 2016;16: 04015029
- [9] Subasi O, Koltuk S, Iyisan R. A numerical study on the estimation of liquefactioninduced free-field settlements by using PM4Sand model. KSCE J Civ Eng 2022;26 (2):673–84. https://doi.org/10.1007/s12205-021-0719-0.
- [10] Lai CG, Bozzoni F, Conca D, et al. Technical guidelines for the assessment of earthquake induced liquefaction hazard at urban scale. Bull Earthq Eng 2021;19: 4013–57. https://doi.org/10.1007/s10518-020-00951-8.
- [11] Molina-Gómez F, Ferreira C, Ramos C, Viana da Fonseca A. Performance of gelpush sampling in liquefiable soils. Géotech Lett 2020;10(2):256–61. https://doi. org/10.1680/jzele.19.00073
- [12] Boulanger RW, Idriss IM. CPT-based liquefaction triggering procedure. J Geotech Geoenviron Eng 2016;142(2):04015065. https://doi.org/10.1061/(ASCE) GT.1943-5606.000138.
- [13] Jamiolkowski M, Lo Presti DCF. DMT research in sand. What can be learned from calibration chamber tests. In: Proc., 1st int conf on site characterization ISC'98. Atlanta: Oral presentation; 1998.
- [14] Lee M, Choi S, Kim M, Lee W. Effect of stress history on CPT and DMT results in sand. J Eng Geol 2011;117:259–65.
- [15] Marchetti S. Incorporating the stress history parameter KD of DMT into the liquefaction correlations in clean uncemented sands. J Geotech Geoenviron Eng 2015;142(2). ASCE.
- [16] Rollins KM, Remund TK, Amoroso S. Evaluation of DMT-based liquefaction triggering curves based on field case histories. In: Proc., 5th international conference on geotechnical and geophysical site characterisation; September 2016. p. 5–9. Queensland, Australia.
- [17] Monaco P, Marchetti S, Totani G, Calabrese M. Sand liquefiability assessment by flat dilatometer test (DMT). Proc., 16th Conf Soil Mech Geotech Eng September 2005;4:2693–7. Osaka.
- [18] Grasso S, Maugeri M. The seismic dilatometer Marchetti test (SDMT) for evaluating liquefaction potential under cyclic loading. Sacramento, CA, USA. In: Proc., IV geotechnical earthquake engineering and soil dynamic; 2008. 978-0-7844-0975-6.
- [19] Tsai P, Lee D, Kung GT, Juang CH. Simplified DMT-based methods for evaluating liquefaction resistance of soils. J Eng Geol 2009;103:13–22.
- [20] Robertson PK. Interpretation of in-situ tests some insight. Mitchell Lecture. Proc., 4th Int Conf Site Charact, ISC-4, Porto de Galinhas 2012;1:3–24. Brazil.

- [21] Andrus R, Stokoe IIKH. Liquefaction resistance of soils from shear-wave velocity. J Geotech Geoenviron Eng 2000;126(11):1015–25. https://doi.org/10.1061/ (ASCE)1090-0241(2000)126:11(1015).
- [22] Grasso S, Maugeri M, Monaco P. Using KD and vs from Seismic Dilatometer (SDMT) for evaluating soil liquefaction. In: Proc., 2nd international conference on the flat dilatometer; 2006. Washington, 2 – 5 April.
- [23] Marchetti S. Detection of liquefiable sand layers by means of quasi-static penetration tests. Proc., 2nd European Symp on Penetration Testing 24-27 May 1982;2:689–95. Amsterdam.
- [24] Totani G, Marchetti S, Monaco P, Calabrese M. Use of the flat dilatometer test (DMT) in geotechnical design. In: Proc., intnl conf on in situ measurement of soil properties, bali, Indonesia; May 2001.
- [25] Yu HS. In situ soil testing: from mechanics to interpretation. 1st J.K. Mitchell Lecture. In: Proc., 2nd int. Conf. On site characterization; 2004. p. 3–38. ISC-2, Porto
- [26] Viana Da Fonseca A. Application of in situ testing in tailing dams, emphasis on liquefaction; case-history. Proc., 4th Int Conf Site Charact, ISC-4, Porto de Galinhas 2012;1:181–203. Brazil.
- [27] Boulanger RW, Ziotopoulou K. Formulation of a sand plasticity plane-strain model for earthquake engineering applications. Soil Dynam Earthq Eng 2013;53:254–67.
- [28] Tasiopoulou P, Gerolymos N. Constitutive modeling of sand: formulation of a new plasticity approach. Soil Dynam Earthq Eng 2016;82:205–21.
- [29] Tsaparli V, Kontoe S, Taborda DMG, Potts DM. A case study of liquefaction: demonstrating the application of an advanced model and understanding the pitfalls of the simplified procedure. Geotechnique 2020;70(6):538–58.
- [30] Petalas A, Galavi V. In: Plaxis liquefaction model UBC3D-PLM; 2012.
- [31] Puebla H, Byrne PM, Phillips R. Analysis of CANLEX liquefaction embankments: prototype and centrifuge models. Can Geotech J 1997;34:641–57.
- [32] Beaty M, Byrne PM. An effective stress model for prediction liquefaction behaviour of sand. Geotech Earth Eng Solid Dynam III 1998;75:766–77. ASCE Geotechnical Special Publication.
- [33] Seed HB, Idriss IM. Simplified procedure for evaluating soil liquefaction potential. J Soil Mech Found Div 1971;97:1249–73.
- [34] Galavi V, Petalas A, Brinkgreve RBJ. Finite element modelling of seismic liquefaction in soils. Geotech Eng J SEAGS & AGSSEA September 2013;44(3). ISSN 0046-5828.
- [35] PLAXIS3D. Material models manual. Available at: https://communities.bentley. com; 2018.
- [36] Quintero J, Carrilho Gomes R, Rios S, Ferreira C, Viana da Fonseca A. Liquefaction assessment based on numerical simulations and simplified methods: a deep soil deposit case study in the Greater Lisbon. Soil Dynam Earthq Eng 2023;169:107261. https://doi.org/10.1016/j.soildyn.2023.10786615.
- [37] Beaty MH, Byrne PM. In: UBCSAND constitutive model, version 904aR, UBCSAND Constitutive model on itasca UDM web site; February 2011.
- [38] Makra A. Evaluation of the UBC3D-PLM constitutive model for prediction of earthquake induced liquefaction on embankment dams. TU Delft; 2013. MSc Thesis.
- [39] Bolton MD. The strenght and dilatancy of sands. Geotechnique 1986;36(1):65-78.
- [40] Mayne PW. Stress-strain-strength-flow parameters from enhanced in-situ tests. In: Proc., international conference on in-situ measurement of soil properties and case histories; 21-24 May 2001. p. 27–47. Indonesia.
- [41] Skempton AW. Standard penetration test procedures and the effects in sands of overburden pressure, relative density, particle size, ageing and overconsolidation. Geotechnique 1986;36(3):425-47.
- [42] Reyna F, Chameau JL. Dilatometer based liquefaction potential of sites in the imperial valley. In: Proc., 2nd int conf on recent adv in geot earthquake engrg and soil dyn; 1991. p. 385–92. St. Louis.
- [43] Tanaka H, Tanaka M. Characterization of sandy soils using CPT and DMT. Soils Found 1998;38(3):55–65.
- [44] TC16 DMT Report 2001. The flat dilatometer test (DMT) in soil investigations. In: A report by the ISSMGE committee TC16. 41 pp. Reprinted in proc. DMT; 2006. Washington D.C.
- [45] Cavallaro A, Grasso S, Sammito MSV. A seismic microzonation study for some areas around the Mt. Etna volcano on the east coast of sicily, Italy. In: Proc., 4th international conference on performance based design in earthquake geotechnical engineering, Beijing, China; 2022. https://doi.org/10.1007/978-3-031-11898-2_ 61.
- [46] Cavallaro A, Fiamingo A, Grasso S, Massimino MR, Sammito MSV. Local site amplification maps for the volcanic area of Trecastagni, south-eastern Sicily (Italy). Bull Earthq Eng 2024;22:1635–76. https://doi.org/10.1007/s10518-023-01834-4.
- [47] Grasso S, Sammito MSV. Uncertainties in performance based design methodologies for seismic microzonation of ground motion and site effects: state of development and applications for Italy. In: Proc., 4th international conference on performance based design in earthquake geotechnical engineering, Beijing, China; 2022. https://doi.org/10.1007/978-3-031-11898-2_23.
- [48] Barreca G, Monaco C. Vertical-axis rotations in the Sicilian fold and thrust belt: new structural constraints from the Madonie Mts. (Sicily, Italy). Ital J Geosci 2013; 132(3):407–21.
- [49] Comerci V, Vittori E, Blumetti AM, Brustia E, Di Manna P, Guerrieri L, Lucarini M, Serva L. Environmental effects of the december 28, 1908, southern calabria–messina (southern Italy) earthquake. Nat Hazards 2015;76:1849–91. https://doi.org/10.1007/s11069-014-1573-x.
- [50] Pirrotta C, Barbano MS, Guarnieri P, Gerardi F. A new dataset and empirical relationships between magnitude/intensity and epicentral distance for liquefaction in central-eastern Sicily. Ann Geophys 2007;50(6):763–74.

- [51] Barreca G, Gross F, Scarfi L, Aloisi M, Monaco C, Krastel S. The Strait of Messina: seismotectonics and the source of the 1908 earthquake. Earth Sci Rev 2021;218: 103685. https://doi.org/10.1016/j.earscirev.2021.103685.ISSN0012-8252.
- [52] Castelli F, Cavallaro A, Ferraro A, Grasso S, Lentini V, Massimino MR. Dynamic characterisation of a test site in Messina (Italy). Ann Geophys 2018;61(2):222.
- [53] Tarquini S, Isola I, Favalli M, Battistini A. TINITALY, a digital elevation model of Italy with a 10 meters cell size. Version 1.0. Istituto Nazionale di Geofisica e Vulcanologia (INGV); 2007. https://doi.org/10.13127/TINITALY/1.0.. [Accessed 31 July 2022].
- [54] Giampiccolo E, Tusa G, Langer H, Gresta S. Attenuation in southeastern sicily (Italy) by applying different coda methods. J Seismol 2002;6:487–501. https://doi. org/10.1023/A:1021150819311.
- [55] Idriss IM, Boulanger RW. SPT-based liquefaction triggering procedures. Davis, CA: Department of Civil and Environmental Engineering, University of California; 2010. p. 259. Report UCD/CGM-10/02.
- [56] Mitchell JK, Lodge AL, Coutinho RQ, Kayen RE, Seed RB, Nishio S, Stokoe KH. In situ test results from four Loma Prieta earthquake liquefaction sites: SPT, CPT,

- DMT and shear wave velocity. Earthquake engineering research center. Berkeley: University of California; 1994. Report No. UCB/EERC-94/04.
- [57] Idriss IM, Boulanger RW. Semi-empirical procedures for evaluating liquefaction potential during earthquakes. In: Proc., 11th IC SDEE/3rd ICEGE, 7–9 january, vol. 1; 2004. p. 32–56. https://doi.org/10.1016/j.soildyn.2004.11.023. Berkeley, CA, USA.
- [58] Petalas A, Galavi V, Brinkgreve RBJ. Validation and verification of A practical constitutive model for predicting liquefaction in sands. In: Proc., 22nd European young geotechnical engineers conference; 25-29 August 2012. p. 167–72. Gothenburg, Sweden.
- [59] El Takch A, Sadrekarimi A, El Naggar MH. Liquefaction behavior of silt and sandy silts from cyclic ring shear tests. In: Proc., 6th international conference on earthquake geotechnical engineering; November 2015. p. 1–4. Christchurch, New Zealand.
- [60] Viana da Fonseca A, Molina-Gómez F, Ferreira C. Liquefaction resistance of TP-Lisbon sand: a critical state interpretation using in situ and laboratory testing. Bull Earthq Eng 2021;21:767–90. https://doi.org/10.1007/s10518-022-01577-8.